Electronic Supplementary Material (ESI) for Green Chemistry.

Supporting Information

Cell-free production of 1,4-butanediol: Cascade design and discovery of novel promiscuous biocatalysts

Process parameters and substrate promiscuity of *Pu*DHT

Prior to utilizing *Pu*DHT in a cell-free synthetic cascade reaction, it is important to first determine its optimum process parameters and substrate proficiency. *Pu*DHT showed an activity in broad pH with the optimum pH at 7.5 to 8.5 (Figure S1A). *Pu*DHT reached its maximum activity at 50 to 55 °C (Figure S1B). Magnesium has been reported to play crucial role for activity of sugar acid dehydratases—D-xylonate dehydratase from *Caulobacter crescentus* (*Cc*XylDHT) and L-arabinonate dehydratase from *Rhizobium leguminosarum* (*Rl*AraDHT).[1] However, recent work showed that manganese as a more suitable cation for *Cc*XylDHT.[2]

Study on the effect of different metal ions on *Pu*DHT revealed that magnesium is the most activating cation followed by cobalt and manganese. Nickel did not further activate nor inhibit *Pu*DHT, whereas calcium, zinc, cadmium, and copper strongly inhibited enzyme activity. With no addition of extra metal ions, *Pu*DHT exhibited 20% of its maximum activity (Figure S1C). This indicated that *Pu*DHT could already bind metal ion, possibly magnesium, which was present in the *E. coli* cytoplasm—the expression host. Treatment with EDTA completely abolished its activity. Addition of up to 50 mM magnesium was not able to restore to its maximum activity after EDTA-pretreatment (Figure S1D). Magnesium also showed crucial effect on the thermostability of *Pu*DHT. Without addition of magnesium, *Pu*DHT quickly lost its activity. *Pu*DHT could still, however, retain >50% of its original activity after being incubated 1 h at 57 °C in the presence of 5 mM magnesium (Figure 1E).

*Pu*DHT demonstrated a broad substrate acceptance. The highest activity and catalytic efficiency was achieved for D-gluconate (Table S1). The activity of *Pu*DHT decreased as the hain length of sugar acid decreases. *Pu*DHT prefers (R)-configuration of OH group at C4 by showing higher activity for D-gluconate than D-galactonate and for D-xylonate than L-arabinonate (Table S1). Similar preference was also reported for *Cc*XylDHT.[1] Interestingly, our previous work showed that *Pu*DHT has higher sequence similarity to *Rl*AraDHT, a dehydratase with a higher preference for (S)-configuration of OH group at C4.[3] Nevertheless, absolute activity for *Pu*DHT is significantly higher than *Cc*XylDHT and *Rl*AraDHT.[1,3] *Pu*DHT showed almost no reactivity toward DHIV ((R)-2,3-dihydroxy-isovalerate), a natural substrate for [Fe-S]-dependent dihydroxy-acid dehydratase (DHAD).[4,5]

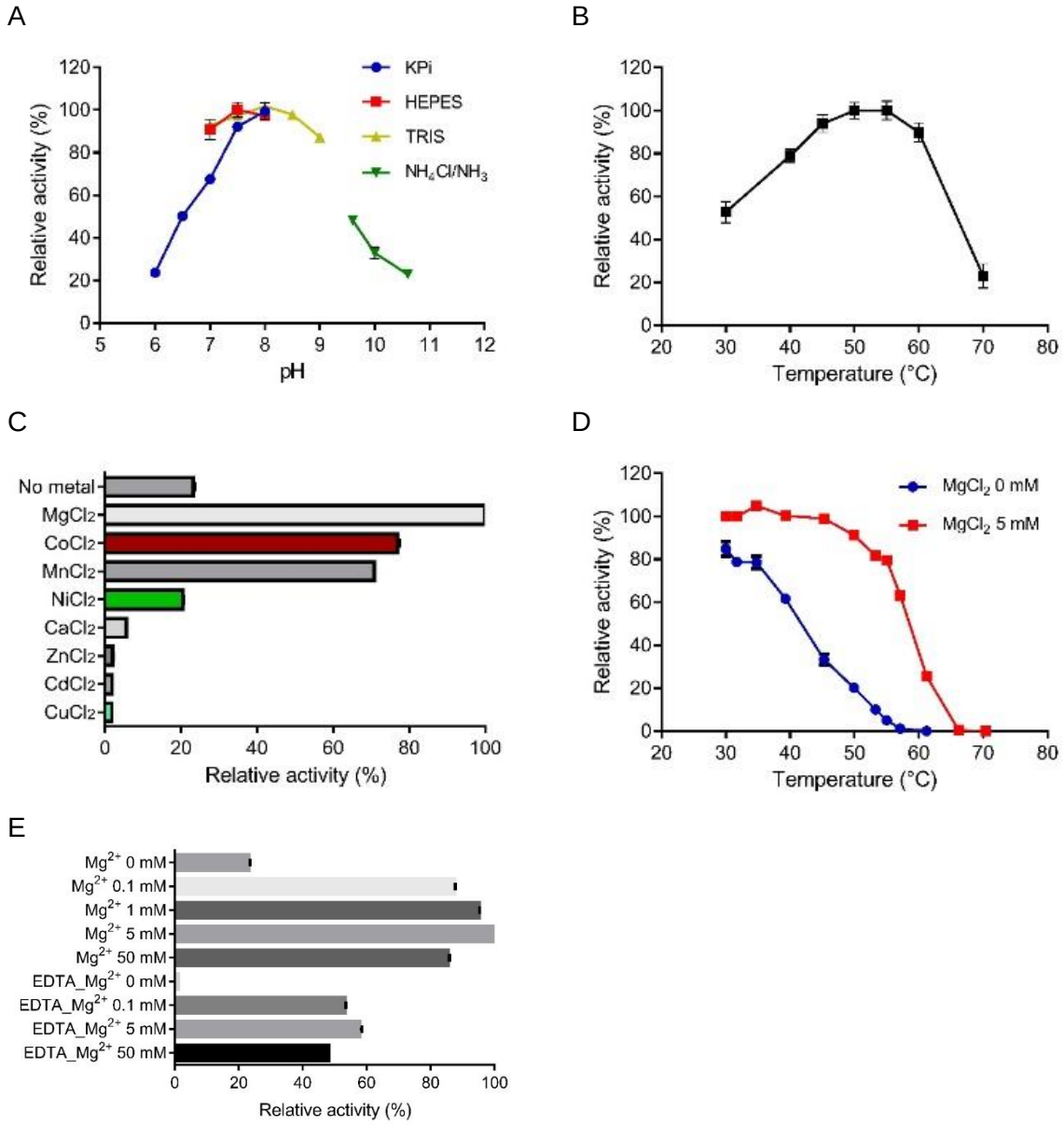

Figure S1. Effect of pH (A), temperature (B), and metal ions (C) on the activity of *Pu*DHT. Kinetic stability of *Pu*DHT in the absence and presence of magnesium (D) and effect of Mg^{2+} concentration and EDTA pretreatment on the initial activity of *Pu*DHT (E). Error bars indicate standard deviation from three independent replications.

Table S1. Substrate promiscuity of *Pu*DHT.*

Substrate	Chemical structure	k_{cat} (s^{-1})	K_M (mM)	k_{cat}/K_M (mM^{-1} s^{-1})	TTN ($x10^3$)
D-Gluconate	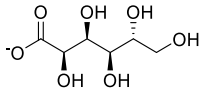	160.4 ± 4.9	5.5 ± 0.6	29.0 ± 3.3	10064 ± 590[3]
D-Galactonate	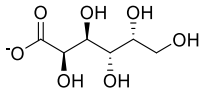	93.3 ± 3.3	3.8 ± 0.4	24.4 ± 2.5	10135 ± 160
D-Xylonate	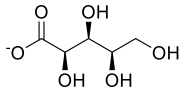	84.3 ± 2.1	3.9 ± 0.4	21.4 ± 2.2	1777 ± 77
L-Arabinonate	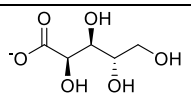	31.5 ± 1.6	7.2 ± 1.2	4.4 ± 0.8	870 ± 48
L-Threonate	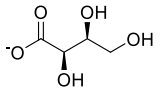	8.1 ± 0.3	6.8 ± 0.9	1.2 ± 0.2	198 ± 48
D-Glycerate	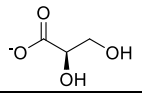	1.4 ± 0.0	7.9 ± 0.9	0.2 ± 0.0	90.5 ± 0.3[3]

* All activity measurements were performed in HEPES 50 mM, pH 7.5 at 50 °C. Error values represent standard deviation from three independent repeats. Non-linear regression of enzyme activity as a function of substrate concentration is presented in Figure S2.

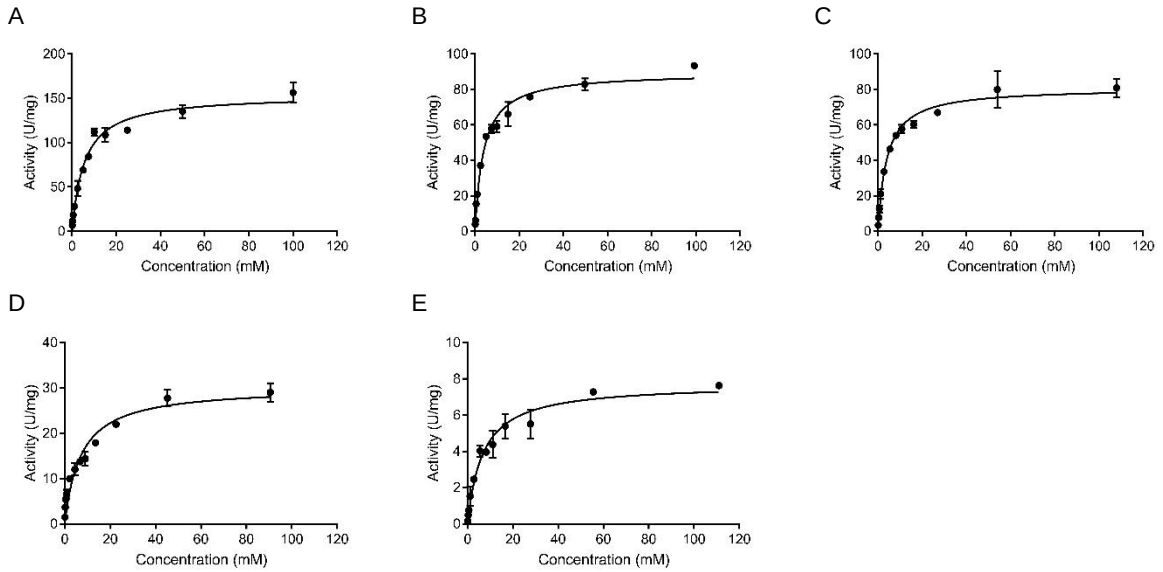

Figure S2. Michaelis-Menten kinetics of *Pu*DHT toward D-gluconate (A), D-galactonate (B), D-xylonate (C), L-arabinonate (D), and L-threonate (E). One unit (U) is defined as the amount of product (µmol) formed per minute. Turnover number (k_{cat}) presented in Table S1 is defined as the number of product formed per enzyme molecule per second. Error bars represent standard deviation from three independent replication. Activity measurement was performed at 50 °C, in HEPES 50 mM pH 7.5.

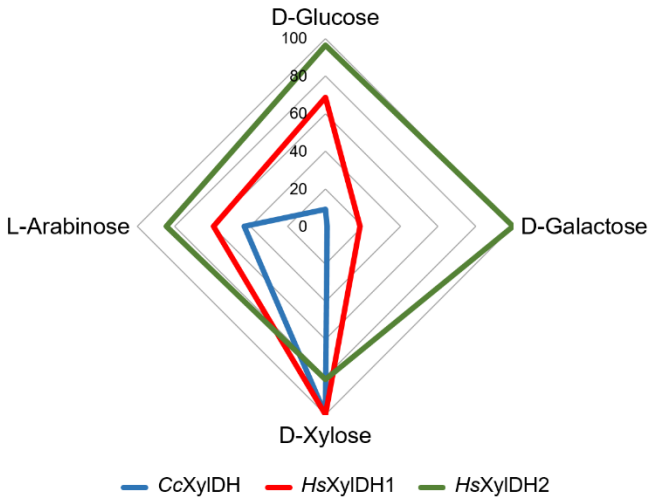

Figure S3. Substrate promiscuity of novel xylose dehydrogenases from *Herbaspirillum seropedicae* (*Hs*XylDH1 and *Hs*XylDH2) in comparison to the xylose dehydrogenase from *Caulobacter crescentus* (XylB, NCBI Reference Number: WP_096032636.1) measured using 25 mM substrates.

Table S2. Kinetic parameters of two putative xylose dehydrogenases from *Herbaspirilum seropedicae* in comparison to the well-characterized xylose dehydrogenase from *Caulobacter crescentus**

Enzyme	Kinetic parameters	D-Glucose	D-Galactose	D-Xylose	L-Arabinose
*Cc*XylDH	V_{max} (U/mg)	5.8 ± 0.1	4.5 ± 1.3	19.3 ± 0.8	13.5 ± 0.7
	K_M (mM)	87.4 ± 3.6	883.8 ± 282.1	0.1 ± 0.1	33.5 ± 3.7
	K_i (mM)[§]	-	-	86.8 ± 18.3	-
*Hs*Xyl1	V_{max} (U/mg)	8,2 ± 0.2	4.2 ± 0.2	11. 2 ± 0.2	10.0 ± 0.2
	K_M (mM)	2,0 ± 0.2	27.3 ± 2.8	0.2 ± 0.0	14.5 ± 0.7
	K_i (mM)[§]	-	-	-	-
*Hs*Xyl2	V_{max} (U/mg)	24.1 ± 0.6	26.5 ± 0.9	18.3 ± 0.5	22.7 ± 0.8
	K_M (mM)	5.9 ± 0.5	0.9 ± 0.1	3.4 ± 0.4	0.4 ± 0.1
	K_i (mM)[§]	-	147.9 ± 25,9	-	128.8 ± 23.4

*All measurements were performed in HEPES pH 7.5, 25 °C, 1 mM NAD^+. Error values are standard deviation from three independent measurement.

[§]Ki is substrate inhibition constant and calculated based on the modified Michaelis Menten kinetics: $V = \frac{V_{max} * S}{K_M * S(1+\frac{S}{K_i})}$. "-" sign indicates no substrate inhibition was observed; thus, standard Michaelis Menten model was used.

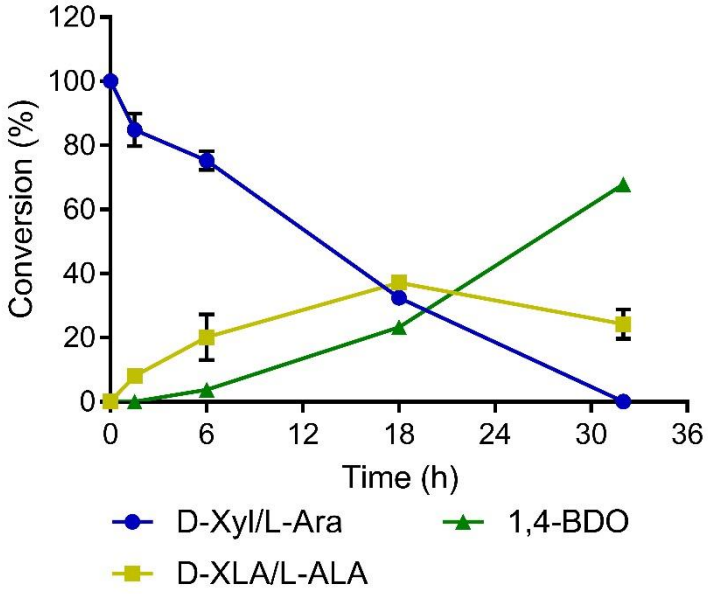

Figure S4. Production of 1,4-butanediol from D-xylose and L-arabinose without lactonase. D-Xyl is D-xylose, L-Ara is L-arabinose, D-XLA is D-xylonolactone, L-ALA is L-arabinolactone, 1,4-BDO is 1,4-butanediol. The biotransformation was performed at 30 °C, 700 rpm. Error bars are standard deviation from three independent measurement.

Discovery of novel promiscuous lactonases

Pentonolactonase from *Haloferax volcanii* is reported to have promiscuous activity toward sugar lactones. However, this enzyme requires high concentration of salt (KCl 1.5 M).[6] Thus, it would be not suitable for biotransformation of D-xylose and L-Arabinose to 1,4-butanediol. We then used the sequence of pentonolactonase from *Haloferax volcanii* to find possible promiscuous lactonases from several microorganisms from which we have cloned either their [Fe-S]-dependent dehydratase of D- or L-2-keto-3-deoxy-pentonate in our previous studies.[3,7] Based on the sequence similarity, we cloned and expressed four lactonases. One lactonase is from *Pseudomonas putida*, three are from *Noviherbaspirillum massilense* (*Nm*Lac1, *Nm*Lac2, and *Nm*Lac3). All of them are annotated to belong to SMP-30/gluconolactonase/LRE family protein. Only *Nm*Lac2 and *Pp*Lac were solubly expressed at standard condition (30 °C, 16 h, autoinduction media) (Figure S6). However, after purification *Pp*Lac precipitated quickly in a desalting buffer (HEPES 50 mM, pH 7.0). We then proceeded with *Nm*Lac2.

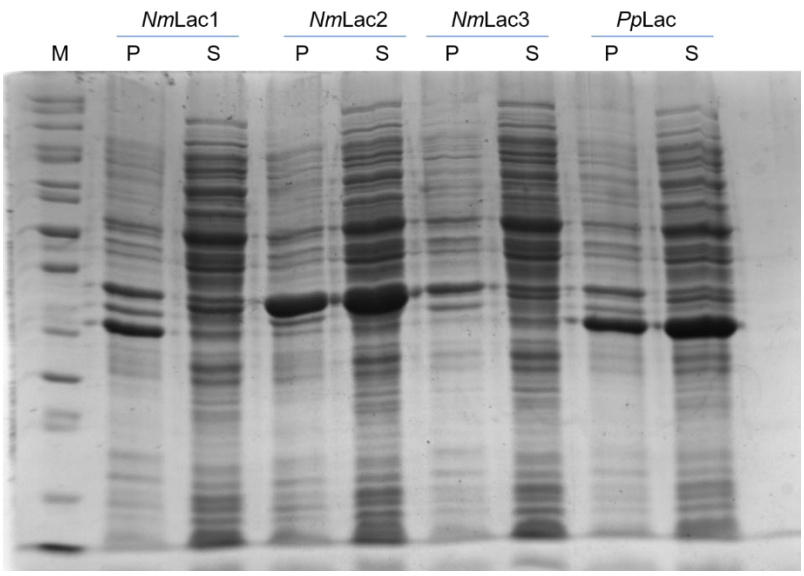

Figure S6. SDS-PAGE gel of lactonases expressed in autoinduction media at 30 °C for 16 h. *Nm* is *Noviherbaspirillum massilense* and *Pp* is *Pseudomonas putida*. M is marker, P is pellet, and S is supernatant.

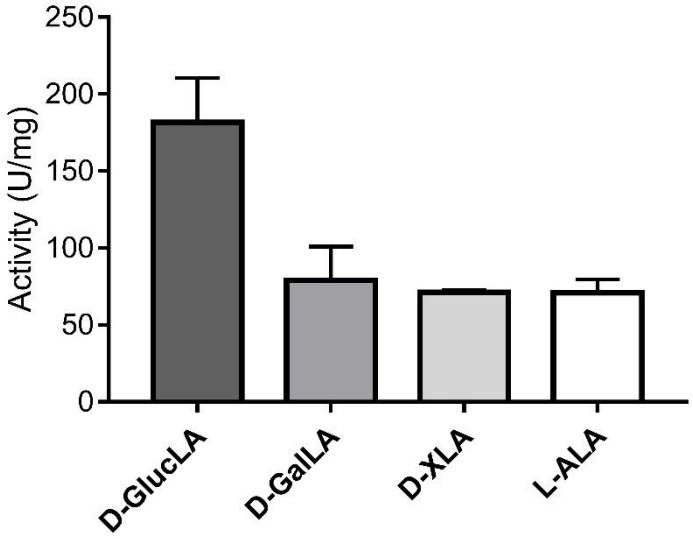

Figure S7 Activity of *Nm*Lac2 toward different sugar lactones at 25°C in HEPES 100 mM pH 7.0. Error bars are standard deviations from three independent replications.

Production of α-ketoglutarate: Application of a "plug-and-play" strategy

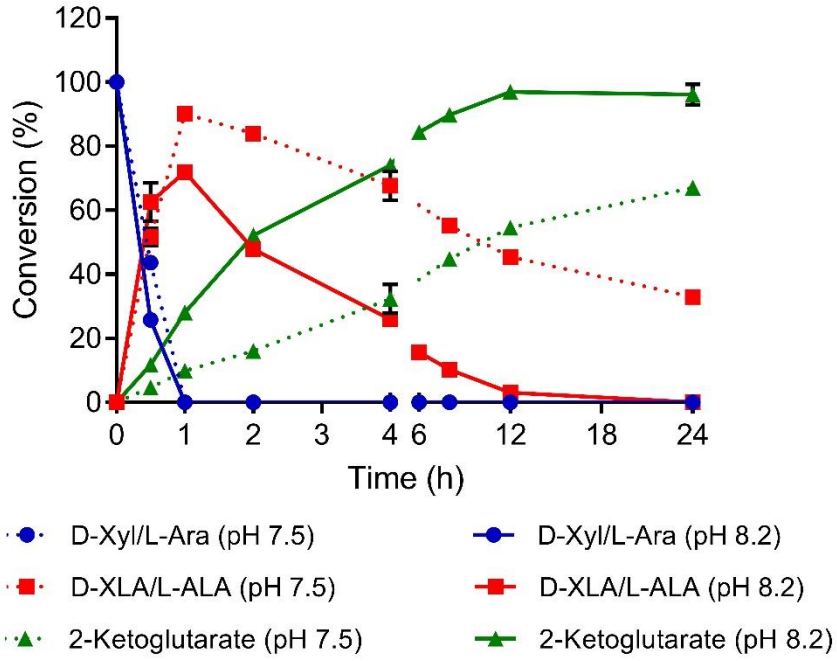

Figure S8. Biotransformation of α-ketoglutarate (2-KG) from D-xylose (D-Xyl) and L-arabinose (L-Ara) at pH 7.5, 25 °C (dotted lines) and at pH 8.2, 30 °C (solid lines) without additional *Nm*Lac2. At higher pH and temperature, significantly faster formation of α-KG was observed due to faster lactones´ opening (D-XLA/L-ALA). D-XLA is D-xylonolactone and L-ALA is L-arabinolactone. Error bars are standard deviations from three independent replications

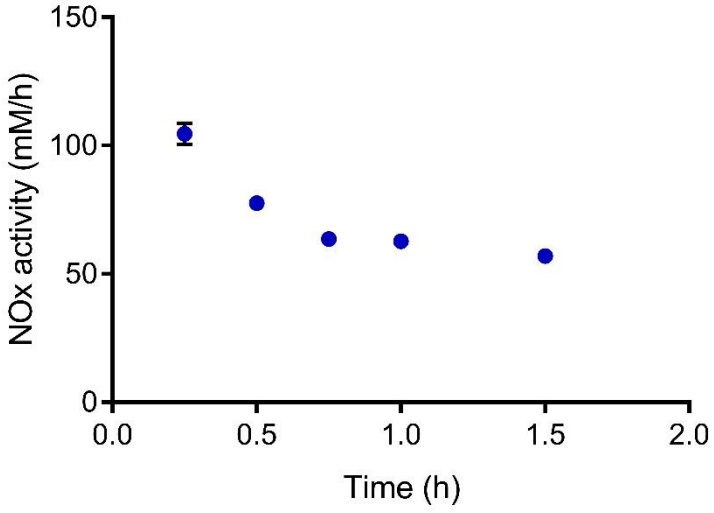

Figure S9. Activity of *Lp*NOX in the optimized condition presented in Figure 2. Activity of the NOX is calculated by summing the concentration of sugar acids and α-ketoglutarate formed and subtracted by initial NAD^+ concentration (5 mM) over time. Error bars represent standard deviations from three independent replications.

Promiscuous enzymes toward third generation chemicals production

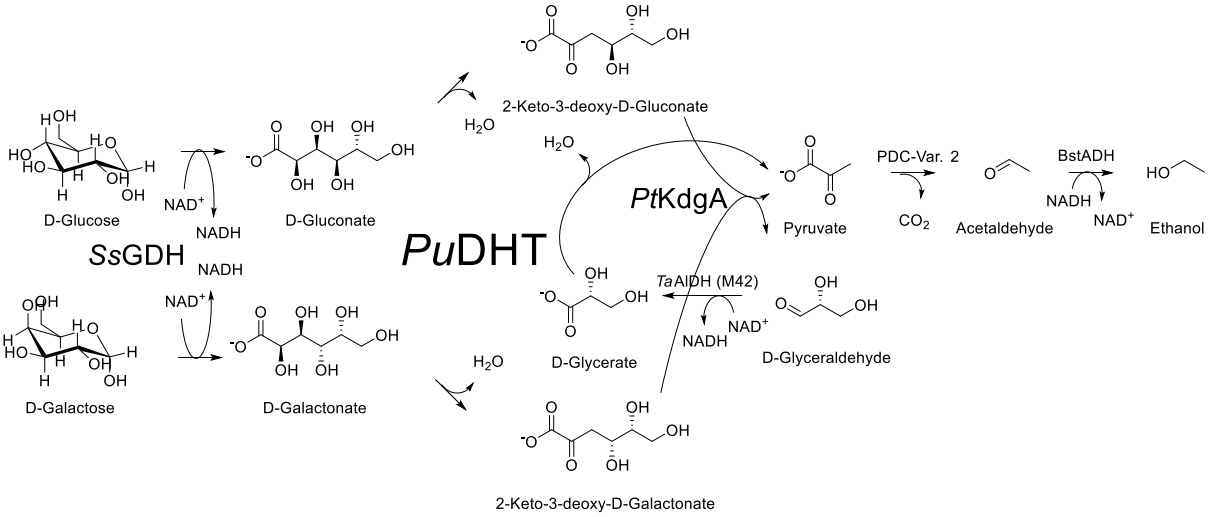

Scheme S1. Cell-free biotransformation of D-glucose and D-galactose to ethanol using three promiscuous enzymes (*Ss*GDH, *Pu*DHT, and *Pt*KdgA). *Pu*DHT also catalysed dehydration of D-glycerate to pyruvate.

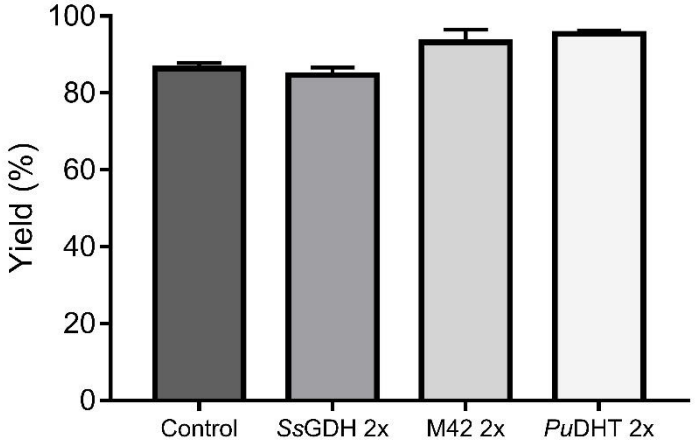

Figure S10. Effect of addition of key enzymes on the ethanol yield after 20 h biotransformation at 50 °C, 700 rpm. Volumetric activity of each enzyme was presented in Materials and Methods.

Table S3. List of the novel promiscuous enzymes

Microorganism	DSMZ number	Enzymes	NCBI Ref. Seq.	Primers (5´→ 3´)*
Herbaspirillum seropediceae Z67	6445	*Hs*XylDH1	WP_013236416.1	F: CAGCAGCATATGACCGCAGCCACCACCCCCGC R: CAGCAGCTCGAGTTACGCGCCCAGCCAGCCGGCATCG
		*Hs*XylDH2	WP_013233071.1	F: CAGCAGCATATGAGCAACACTCCCCAGAACGTGCAACTGG R: CAGCAGCTCGAGTTAGACCCAACCGGCATCGACGATGAATTCCTGC
Noviherbaspirillum massiliense	25712	*Nm*Lac1	WP_081583573.1	F: CAGCAGCATATGCAAGTCGGCGAAAGTCCACTCTGGCATCC R: CAGCAGCTCGAGTTAAGGCTGATAGCTGGGCTCATCAAGACCGGCAATAC
		*Nm*Lac2	WP_051155289.1	F: CAGCAGCATATGGAGAGGCCGATGAAGACTCCGGAGTGTGTC R: CAGCAGCTCGAGTTATGCGGATGTCAGCTCGCTTCGGAAAGTATTGGC
		*Nm*Lac3	WP_019142791.1	F: CAGCAGCATATGTTGCGTAAAGGTCTCGCTGTCATTCTTGTGCTGGTC R: CAGCAGGAATTCTTAGCGCAAGCCGGCTGCGTCCTTGG
Pseudomonas putida KT2440	6125	*Pp*Lac	WP_010952324.1	F: CAGCAGCATATGAACTGCGAACTGATCGTCGACGCCCGC R: CAGCAGCTCGAGTTAGCCCCGGTAGGCAGGTTCCTCCAGG

*Sequence of restriction enzymes is underlined

Table S4. Auxiliary enzymes used in the cascades in this study

Enzyme	Microorganisms	NCBI Ref. Seq.*	Substitution	Reference
*Pu*DHT	*Paralcaligenes ureilyticus*	WP_132585145.1	Wild type	[3]
*Pp*D-KdpD	*Pseudomonas putida*	WP_010953745.1	Wild type	[7]
*Cn*L-KdpD	*Cupriavidus necator*	WP_011616492.1	Wild type	[7]
*Ll*KdcA-Var.1	*Lactococcus lactis*	PDB: 2vbf	Q252N, D306G, E316R, F388Y	[8]
*Ec*Adh Z3 (LND)	*Escherichia coli*	U14003.1	See publication	[9]
*Ec*AdhP	*Escherichia coli*	PDB: 4GKV	Wild type	[10]
*Cb*FDH	*Candida boidinii*		Wild type	[11]
*Pp*KgsaDH	*Pseudomonas putida*	AAN66880.1	Wild type	[12]
*Lp*NOX	*Lactobacillus pentosus*	CCB83530.1	Wild type	[13]
*Ss*GDH	*Saccharalobus solfataricus*	PDB: 2CD9	Wild type	[14]
*Pt*KdgA	*Picrophilus torridus*	WP_048059513.1	Wild type	[15]
*Ta*AlDH (M42)	*Thermoplasma acidophilum*	WP_010901221.1	See publication	[16]
PDC-Var.2	*Acetobacter pasteurianus*	WP_141376382.1	See publication	[17]
*Bst*ADH	*Bacillus stearothermophilus*	KFL15473.1	Wild type	[14]

* The NCBI reference sequences/PDB numbers presented in Table S2 correspond to the wild type sequences

Scaling up the biosynthesis of 1,4-butanediol and α-ketoglutarate: Simple optimization and reaction engineering.

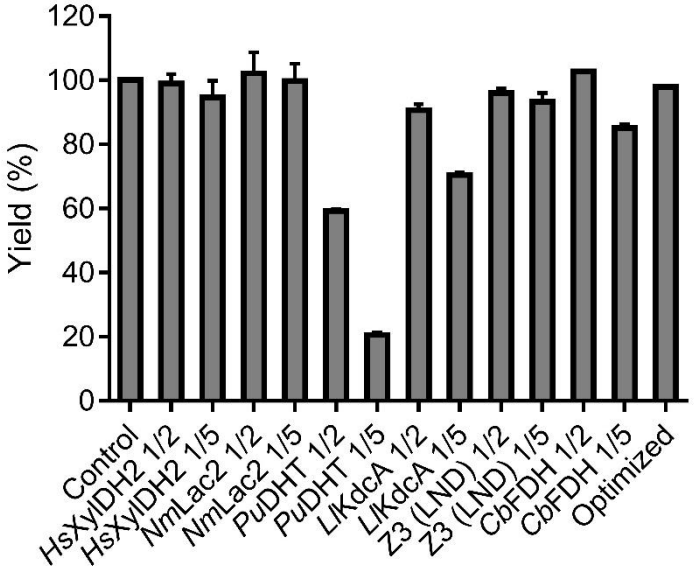

Figure S11. Effect of volumetric activity of each enzyme on the yield of 1,4-butanediol from D-xylose and L-arabinose to 1,4-butanediol after 2 h incubation at 30 °C. Optimized condition contained 50% of *Hs*XylDH2´s volumetric activity (VA), 20% of *Nm*Lac2´s VA, 100% of *Pu*DHT´s VA, 66% of Z3 (LND) and *Cb*FDH´s VA, respectively in comparison to the original reaction (Control).

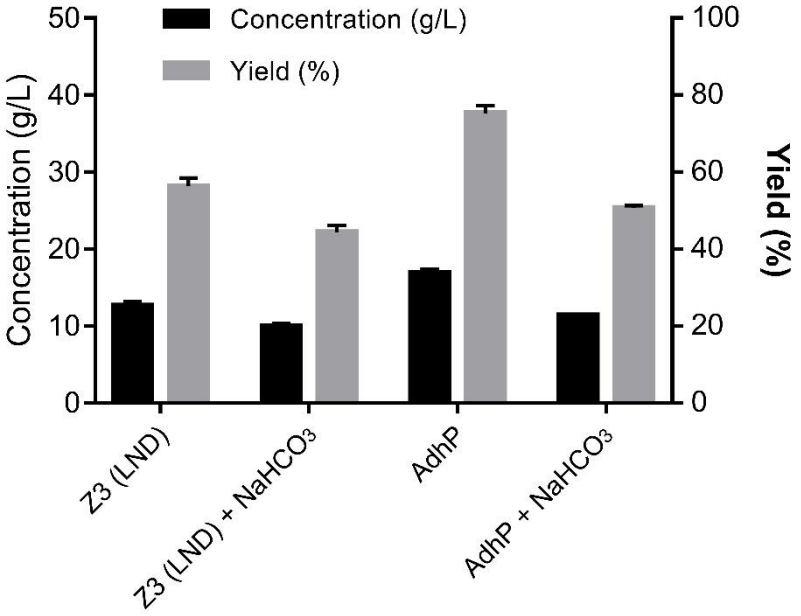

Figure S12. Effect of different alcohol dehydrogenases to the final titer and yield of BDO from 37.5 g/L (250 mM) racemic mixture of D-xylose and L-arabinose after 20 h biotransformation.

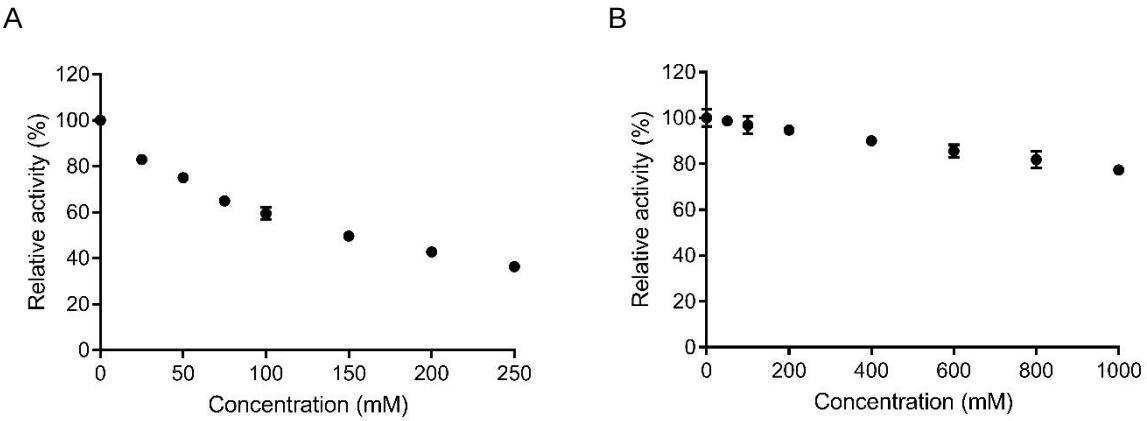

Figure S13. Effect of sodium formate (A) and BDO (B) on *Pu*DHT activity at 25 °C. Activity of *Pu*DHT was measured using direct assay with L-theronate as substrate in HEPES pH 7.5 at 30 °C. Direct assay was performed by monitoring the formation of 2-keto-3-deoxy-L-threonate at 315 nm.

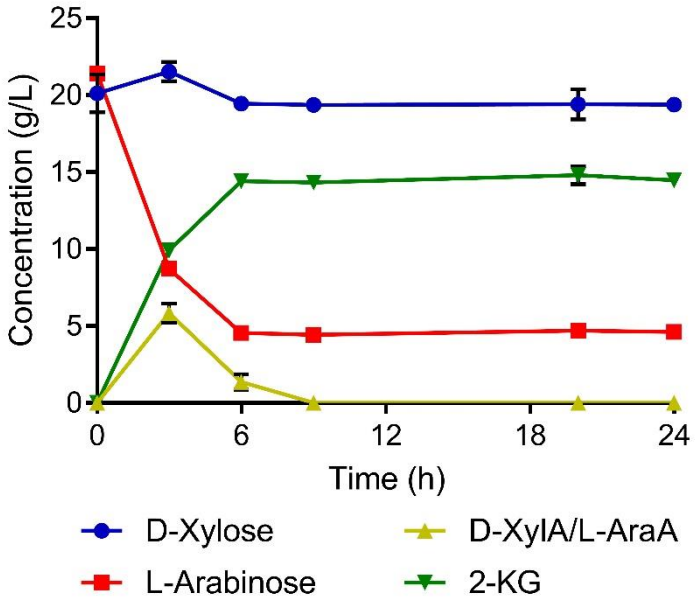

Figure S14. Production of α-ketoglutarate from D-xylose and L-arabinose without addition of *Lp*NOX. The reaction was performed in a nutating compartment system with a breathable sealing containing HEPES 250 mM at 30 °C.

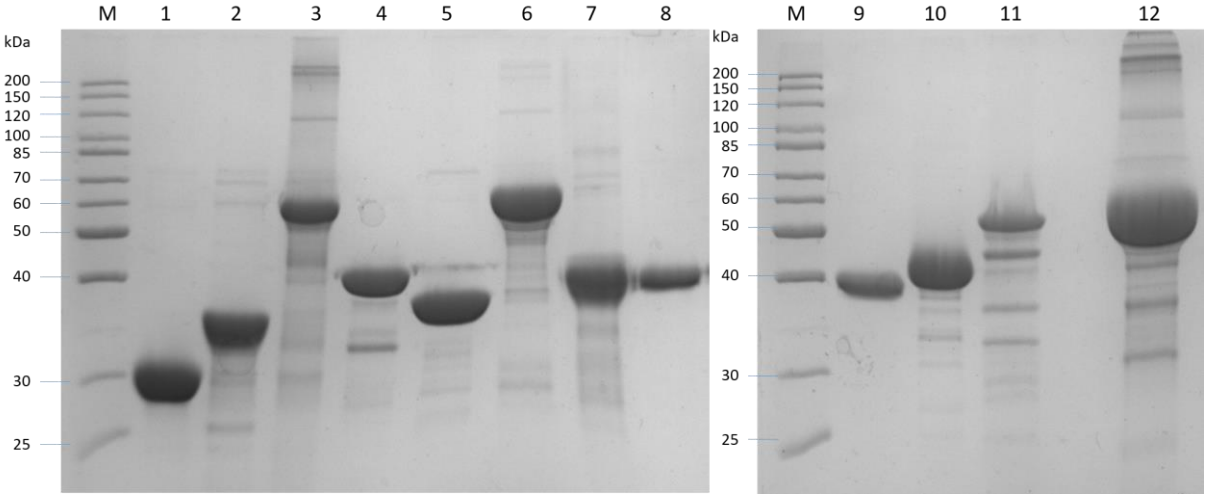

Figure S15. SDS-PAGE of *Pu*DHT and auxiliary enzymes in the biotransformation of D-xylose and L-arabinose. Marker (M), *Hs*XylDH2 (1), *Nm*Lac2 (2), *Pu*DHT (3), *Pp*D-KdpD (4), *Cn*L-KdpD (5), *Ll*KdcA-Var. 1 (6), *Ec*AdhZ3 (LND) (7), *Ec*AdhP (8), *Cb*FDH (9), *Pp*KgsaDH (10), *Lp*NOX (11), protein clumps from the experiment described in Figure S14 (12) are shown.

A

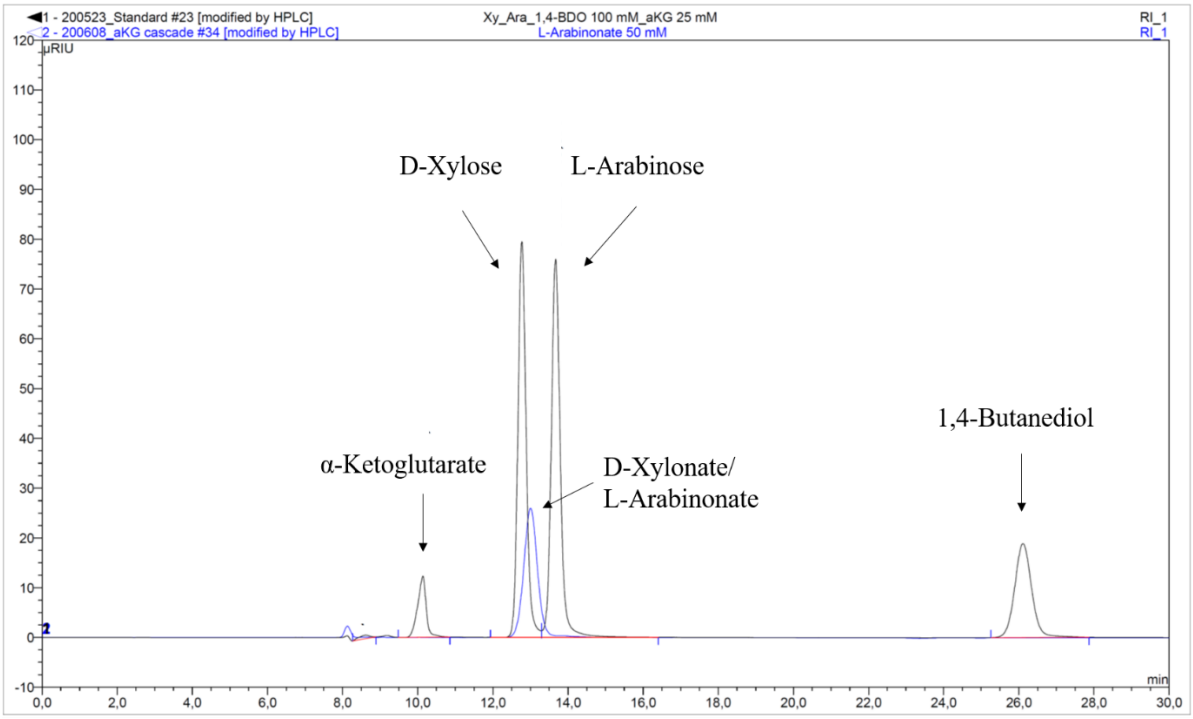

B

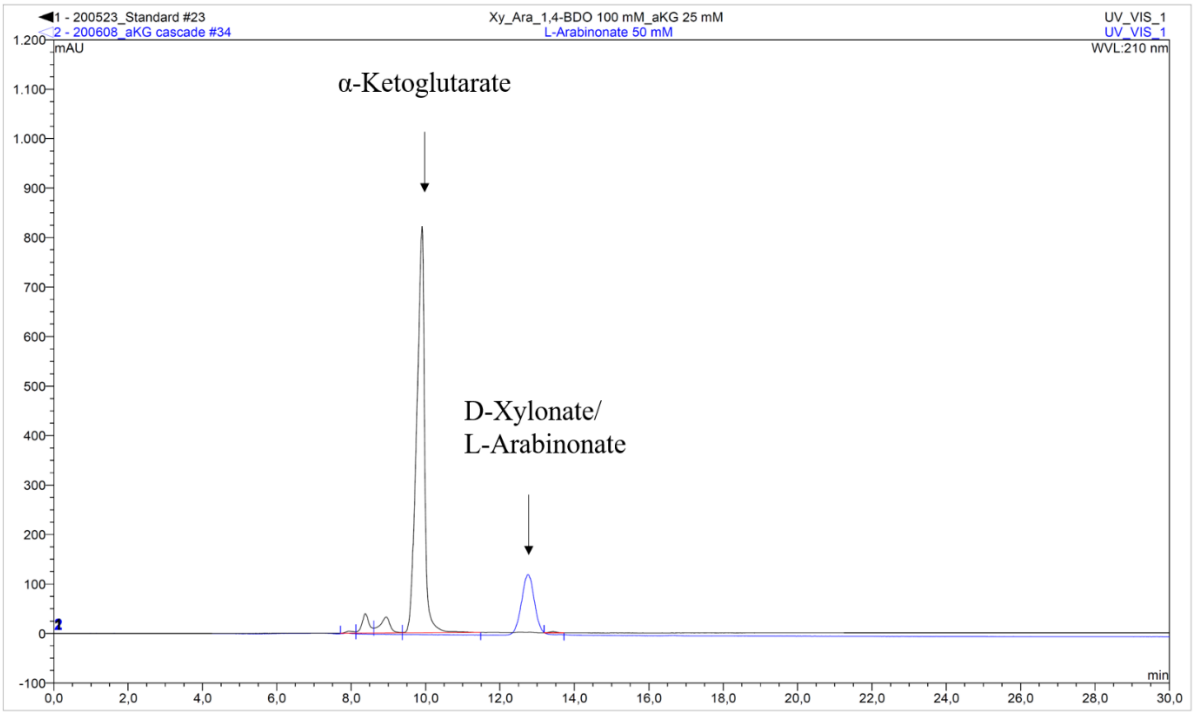

Figure S16. Chromatogram of substrate, intermediate, and product in the biotransformation of D-xylose and L-arabinose with RI detector (A) and UV detector (B).

Materials and Methods

Materials

All materials were purchased as analytical grade or higher from Sigma Aldrich (Darmstadt, Germany) or Carl Roth (Karlsruhe, Germany), unless otherwise stated. All molecular biology reagents including restriction enzymes were purchased from New England Biolab (Frankfurt, Germany). Genomic DNAs were purchased from German Collection of Microorganisms and Cell Cultures (DSMZ).

TTN determination

Total turnover number (TTN) was determined as described previously.[3] In short, diluted *Pu*DHT was incubated in a solution containing HEPES 50 mM pH 7.5, $MgCl_2$ 5 mM, BSA 1 mg/mL, and an appropriate amount of substrate (D-galactonate, D-xylonate, L-arabinonate, and L-threonate). D-galactonate, D-xylonate, and L-arabinonate were produced from the respective sugar using gold catalyst according to the protocol described earlier.[7] L-threonate was purchased as magnesium salt; thus, no additional was $MgCl_2$ added. The reaction solution was incubated in an Eppendorf shaker (500 rpm, ThermoMixer C, Eppendorf, Germany) at 50 °C. An aliquot was taken after 0, 48 h, and 96 h. After appropriate dilutions with water, the solution was filtered through a 10 kDa centrifugal filter (VWR, Germany). The filtrate was subjected to HPLC analysis using an anion exchange column (Metrosep A Supp 16-250, Metrohm, Germany) with a method described before.[3]

Cloning, expression, and protein purification

*Pu*DHT was expressed in TB media and induced using 0.5 mM IPTG (Isopropyl β-D-1-thiogalactopyranoside) as described previously.[3] New promiscuous enzymes were amplified from gDNAs using two-step PCR protocol (PCR without annealing step) according to the protocol described by NEB. Primers used to amplify the genes are listed in Table S3. The genes were digested using appropriate restriction enzymes and cloned to pET28a (Novagen, Germany) bearing N-terminally fused hexahistidines. The newly cloned genes and other auxiliary enzymes (Table S4) were used to transform *E. coli* BL21 (DE3). All auxiliary enzymes were produced in the autoinduction media containing kanamycin 100 µg/mL at 30 °C for 20 h.[18] Purification of *Pu*DHT and the auxiliary enzymes were performed in Äkta purifier using Histrap column FF Crude 5 mL (GE Healthcares, Germany). The buffer was then changed to HEPES 50 mM pH 7.5 using HiPrep desalting column 26/10 50 mL (GE Healthcare, Germany). All purified enzymes were flash frozen in liquid N_2 and stored at -80 °C until further use.

Determination of optimum pH and temperature of *Pu*DHT

Optimum pH of *Pu*DHT was determined by a coupled assay. Reaction solutions contained D-xylonate 25 mM, $MgCl_2$ 5 mM, 1 mM NAD^+, 5 U/mL *Pp*D-KdpD, and 5 U/mL *Pp*KgsaDH in an appropriate buffer and pH. Formation of the dehydration product, 2-keto-3-deo-D-xylonate was dehydrated further by *Pp*D-KdpD to form 2-ketoglutaratesemialdehyde (KGSA), which was oxidized by *Pp*KgsaDH to produce 2-ketoglutarate and NADH. The amount of *Pp*D-KdpD and *Pp*KgsaDH used was adjusted in excess so that their activity was not the limiting factor during coupled assay. Reaction was performed in triplicates, at 25 °C. Formation of NADH was measured at 340 nm in Multiskan (Thermo Fischer, Germany).

Optimum temperature of *Pu*DHT was determined by incubating the enzyme with D-gluconate 50 mM, $MgCl_2$ 5 mM in HEPES 50 mM pH 7.5 at appropriate temperatures for 30 min. The reaction solution was incubated in the Eppendorf shaker at 50 °C, 500 rpm. An aliquot was then diluted using water and filtered through 10 kDa column. The product formed, 2-keto-3-deoxy-D-gluconate, was measured using HPLC according to the method described previously.[3]

Effect of metal ions on *Pu*DHT

Activity of *Pu*DHT in the presence of different metal ions as well as the concentration of $MgCl_2$ was determined using HPLC. Reaction solution contained *Pu*DHT, appropriate concentration of metal ion, D-gluconate 50 mM in HEPES 50 mM pH 7.5 and incubated for 30 min in the Eppendorf thermoblock at 50 °C, 500 rpm. The sample was treated as described earlier. The product formed, 2-keto-3-deoxy-D-gluconate, was measured using HPLC according to the method described previously.[3]

For EDTA pretreatment experiment, *Pu*DHT was desalted in HEPES 50 mM, pH 7.5 containing EDTA 5 mM. After 1 h incubation at 25 °C, EDTA was removed using a PD-10 desalting column (GE Healthcare, Germany). Metal-free *Pu*DHT was flash frozen at –80°C prior to further use.

Kinetic characterization of *Pu*DHT toward different sugar acids

Activity of *Pu*DHT as a function of substrate concentration was determined according to the protocol described previously.[3] In short, *Pu*DHT was incubated in HEPES 50 mM pH 7.5, $MgCl_2$ 5 mM, BSA 1 mg/mL, with appropriate substrates and concentrations. For D-gluconate, D-galactonate, D-xylonate, and L-arabinonate final concentration of *Pu*DHT was 1 µg/mL and for L-threonate was 2.5 µg/mL. The experiment was started by addition of enzyme. The reaction solution was incubated in a sealed 96-wells PCR plate. The plate was incubated in a PCR machine and the temperature was set to 50 °C. An aliquot was taken at 0, 15, and 30 min and stopped by filtering through a 10 kDA filter plate centrifugal (AcroPrep™ Advance, VWR, Germany). The substrates (sugar acids) and products (2-keto-3-deoxy-sugar acids) were analyzed by a standard HPLC methods described before.[3,19]

Biotransformation of D-xylose and L-arabinose

For production of 1,4-butanediol (BDO) from both pentoses, the reaction was run at 30 °C in the Eppendorf thermoblock at 700 rpm. The reaction contained *Hs*XylDH2 (8.1 U/mL and 6.5 U/ml for L-arabinose and D-xylose, respectively), *Pu*DHT (4 U/mL and 10.8 U/ml for L-arabinonate and D-xylonate, respectively), *Pp*D-KdpD (1.4 U/mL), *Cn*L-KdpD (5.6 U/mL), *Ll*KdcA-Var. 1 (1.6 U/mL), *Ec*AdhZ3 (LND) (107.4 U/mL measured toward glutaraldehyde)[20], *Cb*FDH (4.3 U/mL), NAD^+ 1 mM, TDP 0.2 mM, $MgCl_2$ 5 mM, D-xylose 25 mM, L-arabinose 25 mM, sodium formate 50 mM, HEPES 250 mM pH 7.5. The reaction was followed over time by taking an aliquot and diluted 10-fold in H_2SO_4 5 mM prior to filtration through the 10 kDA centrifugal column to stop the reaction. The filtrate was analyzed using HPLC using an ion-exclusion column (RezexROA-Organic Acid H+(8%, Phenomenex, Germany) run isocratically using H_2SO_4 2.5 mM at 70 °C for 30 min. Substrates, intermediates, and product were detected using a UV and RI detector. Compound separation profile is presented in Figure S16. After having identified that the lactone-opening reaction as the bottleneck (Figure S4), we added *Nm*Lac2 (10.6 U/mL toward D-xylonolactone and L-arabinolactone) and rerun the reaction as

described above. The improved cascade reaction was presented in Figure 1. Three independent replications were performed.

For production of α-ketoglutarate (2-KG), the reaction was run in a 50 ml falcon tube on a nutating shaker (VWR Rocking Platform, VWR, Germany) 50 rpm. The reaction contained *Hs*XylDH2 (3.6 U/mL and 2.9 U/mL for L-arabinose and D-xylose, respectively), *Pu*DHT (1.8 U/mL and 4.7 U/mL for L-arabinonate and D-xylonate, respectively), *Pp*D-KdpD (1.4 U/mL), *Cn*L-KdpD (5.6 U/mL), *Pp*KgsaDH (5.7 U/mL), *Lp*NOX (7.3 U/mL), NAD^+ 1 mM, $MgCl_2$ 5 mM, D-xylose 25 mM, L-arabinose 25 mM, in HEPES 250 mM pH 7.5. The same sample preparation and analysis were performed as described above. *Nm*Lac2 (4.7 U/mL toward D-xylonolactone and L-arabinolactone) was added to speed up the production formation rate presented in Figure S8. The improved cascade reaction was presented in Figure 2. Three independent replications were performed.

Biotransformation of D-glucose and D-galactose to ethanol

Production of ethanol from D-glucose and D-galactose was adapted from a previous work.[3] The reaction solution contained *Ss*GDH (3 U/mL toward D-glucose/D-galactose), *Pu*DHT (1.5 U/mL toward D-glycerate), *Pt*KdgA (2 U/mL), *Ta*AlDH (M42) (1.2 U/mL)[16], PDC-Var. 2 (12 U/mL)[17], *Bst*ADH (12 U/mL), TDP 0.2 mM, MgCl2 5 mM, NAD^+ 5 mM, D-glucose 25 mM, and D-galactose 25 mM in HEPES 50 mM, pH 7.5. The reaction was initiated by addition of NAD^+. The result of the first cascade adaptation was presented in Figure S10 (Control). After 20 h biotransformation, an aliquot was taken and diluted with H_2SO_4 5 mM prior to filtration through the 10 kDa centrifugal column. Ethanol yield was analyzed according to the previous work.[3] Time course experiment (Figure 3) was run using the same condition, except *Pu*DHT´s volumetric activity was doubled. Three independent replications were performed. The result was presented in Figure 3.

Scaling up for the biotransformation of D-xylose and L-arabinose

For scaling up experiment toward production of BDO, an optimized enzyme concentration (Figure S11) was used. The same reaction condition described earlier was used except the substrate load (D-xylose amd L-arabinose) was increased to 37.5 g/L (250 mM). Concentration of co-substrate sodium formate was also increased to 250 mM. After 20 h biotransformation, BDO yield was measured using the standard HPLC method described earlier. The yield was further improved by replacing *Ec*Adh Z3 (LND) to *Ec*AdhP. Because succinaldehyde was not available commercially, equal concentration of *Ec*AdhP was used for comparison (Figure S12). Time course experiment was performed using *Ec*AdhP and the substrate load was 40 g/L. An aliquot was withdrawn at certain sampling points and subjected to the same pretreatment and HPLC analysis. Three independent replications were performed. The result was presented in Figure 4A.

For the production of 2-KG, the same reaction mix as described earlier was also used. The substrate load was increased to 40 g/L. The reaction was followed over time and the pH was adjusted periodically using 10 M KOH. As presented in Figure S14, the production of 2-KG stopped after 6 h. To increase the yield further, *Lp*NOX (7.3 U/mL) was added two times (after 3 h and 6 h) as well as an appropriate amount of 10 M KOH for pH adjustment. Three independent replications were performed. The result was presented in Figure 4B.

References

1 M. Andberg, N. Aro-kärkkäinen, P. Carlson, M. Oja, S. Bozonnet, M. Toivari, N. Hakulinen and M. O. Donohue, *Appl. Microbiol. Biotechnol.*, 2016, **100**, 7549–7563.

2 L. Shen, M. Kohlhaas, J. Enoki, R. Meier, B. Schönenberger, R. Wohlgemuth, R. Kourist, F. Niemeyer, D. van Niekerk, C. Bräsen, J. Niemeyer, J. Snoep and B. Siebers, *Nat. Commun.*, 2020, **11**, 1–13.

3 S. Sutiono, M. Teshima, B. Beer, G. Schenk and V. Sieber, *ACS Catal.*, 2020, **10**, 3110–3118.

4 M. C. Pirrung, H. joon Ha and C. P. Holmes, *J. Org. Chem.*, 1989, **54**, 1543–1548.

5 H. Gao, T. Azam, S. Randeniya, J. Couturier, N. Rouhier and M. K. Johnson, *J. Biol. Chem.*, 2018, **293**, 4422–4433.

6 J. M. Sutter, U. Johnsen and P. Schönheit, *FEMS Microbiol. Lett.*, 2017, **364**, 1–8.

7 S. Sutiono, B. Siebers and V. Sieber, *Appl. Microbiol. Biotechnol.*, 2020, **104**, 7023–7035.

8 S. Sutiono, J. Carsten and V. Sieber, *ChemSusChem*, 2018, **11**, 3335–3344.

9 A. Pick, W. Ott, T. Howe, J. Schmid and V. Sieber, *J. Biotechnol.*, 2014, **189**, 157–165.

10 L. M. Thomas, A. R. Harper, W. A. Miner, H. O. Ajufo, K. M. Branscum, L. Kao and P. A. Sims, *Acta Crystallogr. Sect. F Struct. Biol. Cryst. Commun.*, 2013, **69**, 730–732.

11 H. Slusarczyk, S. Felber, M. R. Kula and M. Pohl, *Eur. J. Biochem.*, 2000, 267, 1280–1289.

12 B. Beer, A. Pick and V. Sieber, *Metab. Eng.*, 2017, **40**, 5–13.

13 C. Nowak, B. Beer, A. Pick, T. Roth, P. Lommes and V. Sieber, *Front. Microbiol.*, 2015, **6**, 1–9.

14 J. K. Guterl, D. Garbe, J. Carsten, F. Steffler, B. Sommer, S. Reiße, A. Philipp, M. Haack, B. Rühmann, A. Koltermann, U. Kettling, T. Brück and V. Sieber, *ChemSusChem*, 2012, **5**, 2165–2172.

15 T. J. Gmelch, J. M. Sperl and V. Sieber, *Sci. Rep.*, 2019, **9**, 11754.

16 T. J. Gmelch, J. M. Sperl and V. Sieber, *ACS Synth. Biol.*, 2020, **9**, 920–929.

17 S. Sutiono, K. Satzinger, A. Pick, J. Carsten and V. Sieber, *RSC Adv.*, 2019, **9**, 29743–29746.

18 F. W. Studier, *Protein Expr. Purif.*, 2005, **41**, 207–234.

19 J. M. Sperl, J. M. Carsten, J. K. Guterl, P. Lommes and V. Sieber, *ACS Catal.*, 2016, **6**, 6329–6334.

20 A. Pick, B. Rühmann, J. Schmid and V. Sieber, *Appl. Microbiol. Biotechnol.*, 2013, **97**, 5815–5824.